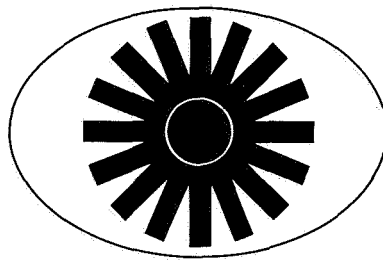


N 69-37973
NASA CR-66836

CASE FILE COPY



TEES

TEXAS ENGINEERING EXPERIMENT STATION
TEXAS A & M UNIVERSITY
COLLEGE STATION TEXAS 77843

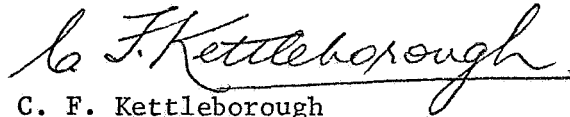
STATUS REPORT TO NATIONAL AERONAUTICS
AND SPACE ADMINISTRATION

Improvement of Propeller Static
Thrust Estimation

NASA Research Grant No. NGR-44-001-011

Report for Period
November 1, 1968 to August 31, 1969

Prepared by

A handwritten signature in cursive script, reading "C. F. Kettleborough". The signature is written in dark ink and is positioned above the printed name and title.

C. F. Kettleborough
Research Associate

August 1969

Submitted by

Texas Engineering Experiment Station
Texas A&M University
College Station, Texas

Abstract

This report describes further feasibility studies of the means of measuring the aerodynamic loading on the blade. The use of micro-miniature pressure transducers has been shown to be unsatisfactory in view of the sensitivity of the transducers to high g loadings parallel to the plane of the transducer diaphragm and high cost. An alternative has been investigated using small bore thin-walled stainless steel tube. Some preliminary studies are reported using the Biot-Savart Law to determine the induced velocities.

IMPROVEMENT OF PROPELLER STATIC THRUST ESTIMATION

Experimental

Efforts have continued to design propeller blades and propeller blade instrumentation to permit collecting data regarding the local pressures that exist at the blade surface during operation in the static thrust condition. Test blades have been redesigned to a thicker section than previously suggested in order to provide greater stiffness and structural integrity of the blade by virtue of a larger cross section. The general operating limit for the new blades involves a tip speed of 600 feet per second and should not result in excessive loads or stress levels even where the propeller blade surface has been grooved to accept pneumatic tubing. An evaluation of the originally proposed scheme of acquiring blade surface pressures by use of micro-miniature pressure transducers was discontinued in view of the sensitivity of the transducers to high g loadings parallel to the plane of the transducer diaphragm. In addition, the cost of providing an adequate number of transducers as well as the attendant signal conditioning and switching hardware would involve a rather large expenditure of funds which seem disproportionate in view of the anticipated use of the equipment.

The second alternative has been pursued wherein small bore thin-walled stainless steel tubing will be bonded into grooves machined in the blade surfaces and imbedded to a depth equal to the diameter of the tubing. The present design involves the use of a tube having an outside diameter

of .040 inches. Flattened or oblong tubing was available but the cost was excessive in view of the rather small amount of tubing required to instrument the propeller blade. The ends of the imbedded tubing will be sealed and holes drilled into the bore of the tube through the wall normal to the surface at the required point of measurement. All four blades will be instrumented in order to reduce the number of grooves necessary for each blade.

The tubing will be routed through a hole in the shank end of the blade into the hollow portion of the propeller hub where the tubing will be connected to the in-ports of a scani-valve assembly. By means of a slip-ring assembly and suitable instrumentation the pressures are logged on a digital recorder.

Theoretical

Earlier approaches have been based on the Navier-Stokes equations. Attention has now been turned to the application of the Biot-Savart law. The circulation Γ can be expressed as

$$\Gamma = A(r-r_h)^\eta (r_p-r)^\beta \quad (1)$$

The variation in circulation for the case of $\eta=0.75$ and $\beta=0.25$ is shown in figure 1. Superimposed on this graph are five rectangular uniform loadings of varying length but of constant strength equal to $\frac{\Gamma_{\max}}{5A}$. The lengths of the rectangular areas are determined so that the sum of the areas of the five rectangular sections equals the area under the actual loading distribution curve. The induced velocities due

to the ten helical trailing vortices can now be calculated by summation using the Biot-Savart Law.

Figure 2 shows the induced velocities for $\eta=0.75$ and $\beta=0.25$. Figure 3 shows the induced velocities for $\eta=0.5$ and $\beta=0.5$. For both loading configurations considered the axial induced velocity becomes negative inboard of the propeller blade tip. The loading for $\eta=0.5$ and $\beta=0.5$ produced a negative axial velocity at the propeller center as well as at the propeller tip. This condition, i.e. reversal of the axially induced velocity at the center and/or tip, has been observed in experimental studies. From these results it appears that moving the point of maximum aerodynamic loading inboard tends to reduce thrust and increase the area of the propeller plane which experiences a negative induced velocity.

Figures 4 and 5 show how the thrust varies along the blade and illustrate that negative axial velocities seriously reduced the available thrust.

Figures 1 through 5 were obtained by Mr. E. M. Kelley as part of his M. S. thesis.

Nomenclature

A	constant in equation (1)
r	radius
r_h	propeller hub radius
r_p	propeller radius
r, θ, z	cylindrical coordinates
T	thrust
u, v, w	velocities in r, θ, z direction respectively
u_i, v_i, w_i	induced velocities at the propeller plane
η, β	constants in circulation equation (1)
Γ	circulation
Γ_{TV}	tip vortex strength

The normalized variable are defined by

$$\bar{u}_i = \frac{4\pi}{A \Gamma_{TV}} u_i \quad ; \quad \bar{v}_i = \frac{4\pi}{A \Gamma_{TV}} v_i \quad ; \quad \bar{w}_i = \frac{4\pi}{A \Gamma_{TV}} w_i$$

$$T = \frac{8\pi}{\rho A^2 \Gamma_{TV}} \bar{T} \quad ; \quad \bar{T} = \int_{r_h}^{r_p} r \bar{w}_i^2 dr$$

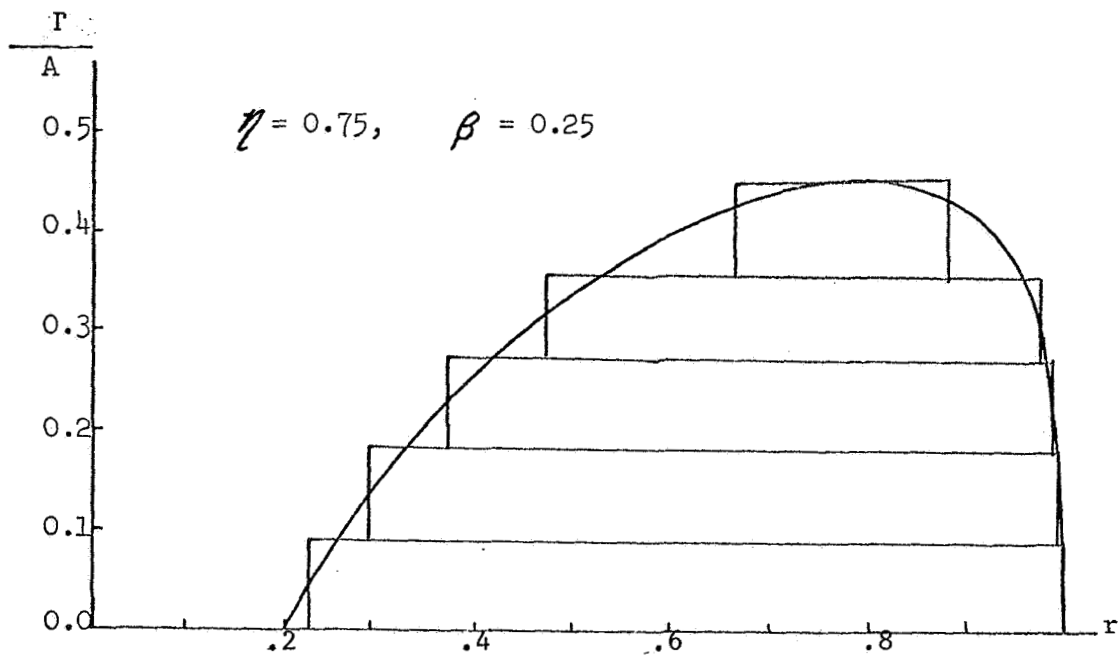


Fig. 1 Blade Circulation

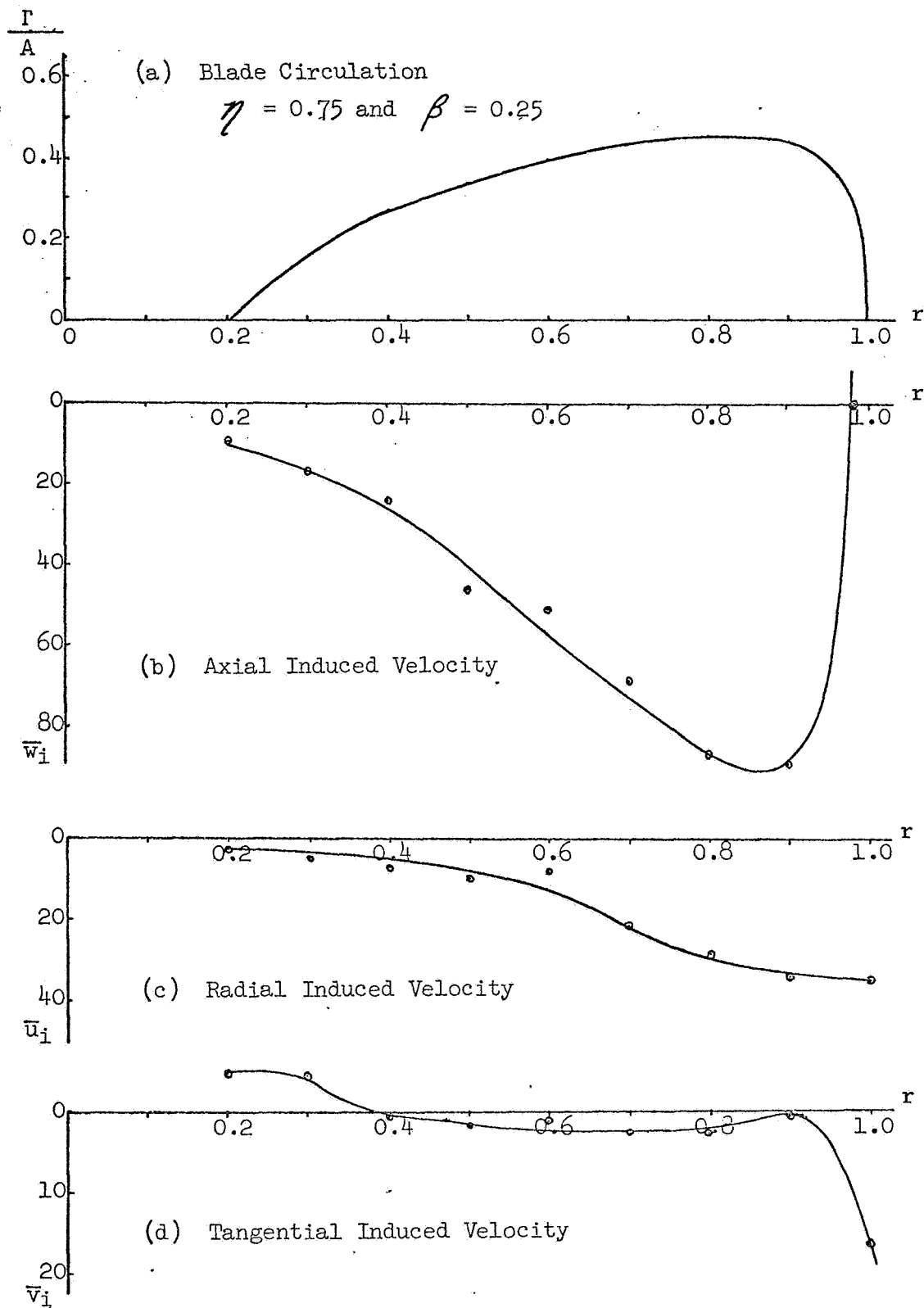


Fig. 2 Trailing Vortex Induced Velocities and Blade Circulation, $\eta = 0.75$ and $\beta = 0.25$

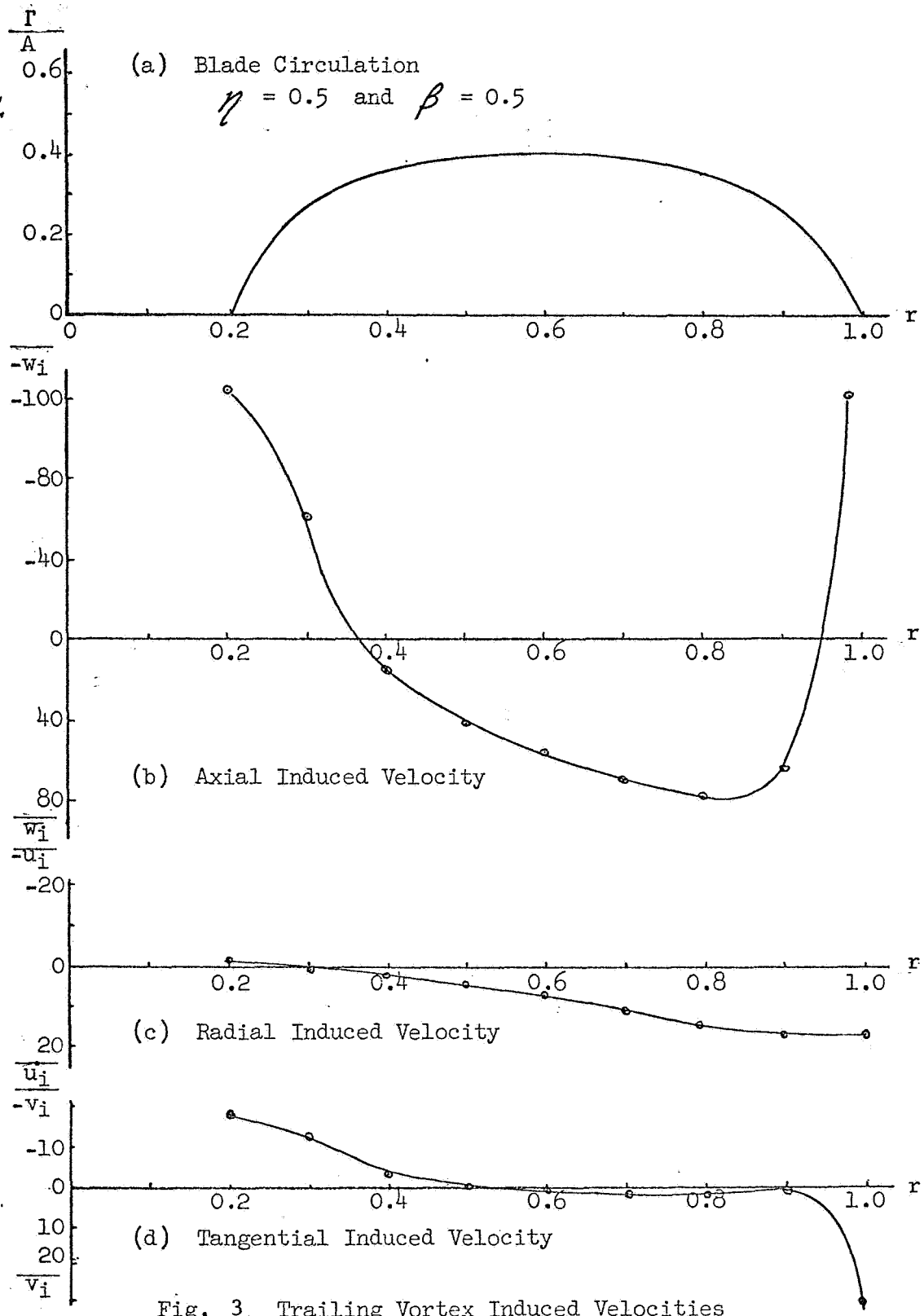


Fig. 3. Trailing Vortex Induced Velocities and Blade Circulation, $\eta = 0.5$ and $\beta = 0.5$

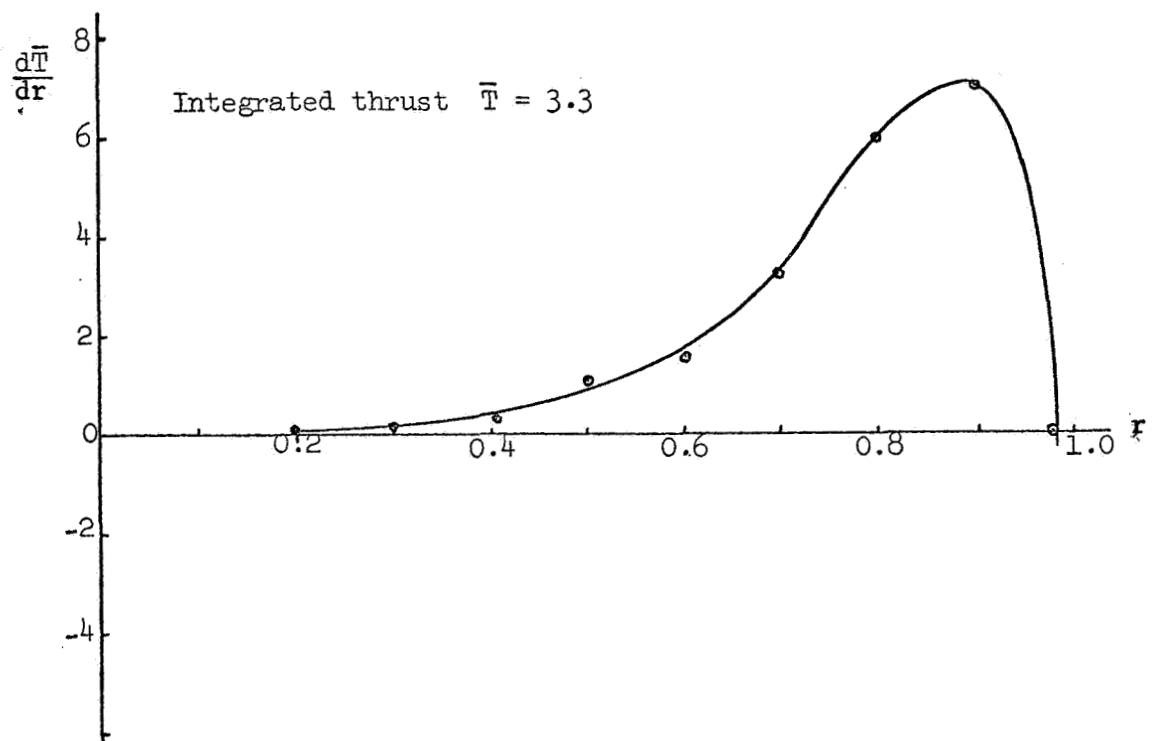


Fig. 4 Thrust Distribution, $\eta = 0.75$ and $\beta = 0.25$

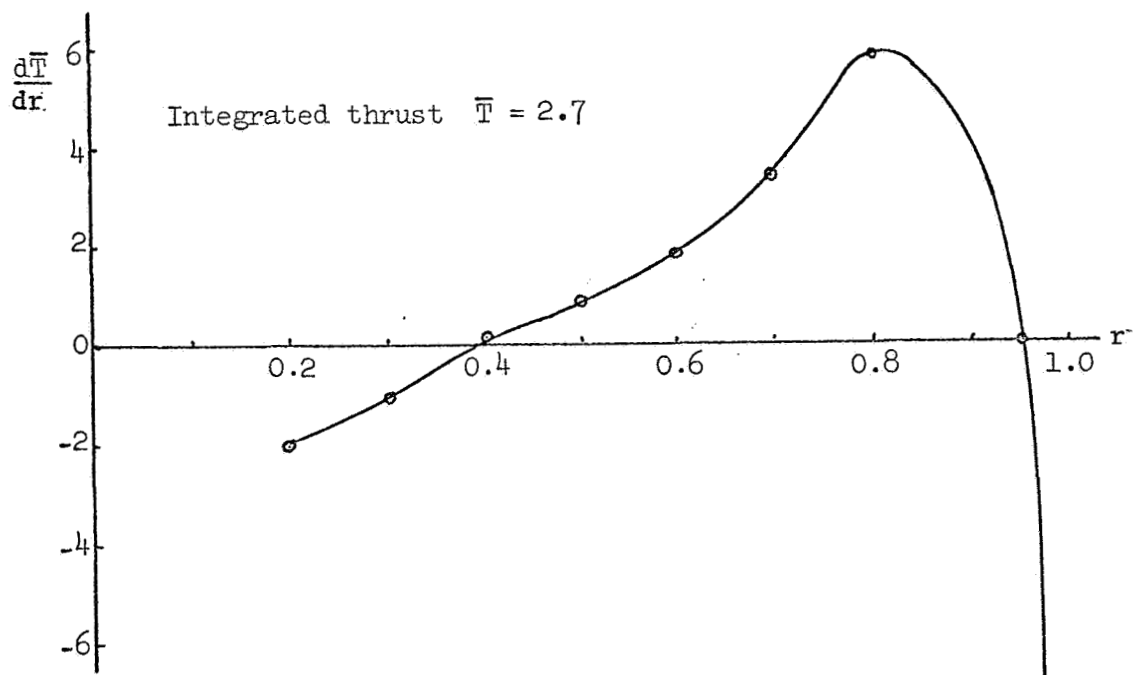


Fig. 5 Thrust Distribution, $\eta = 0.5$ and $\beta = 0.5$